

A robust pedestrian navigation algorithm with low cost IMU

Yan Li

Faculty of Engineering and Information Technology
University of Technology, Sydney (UTS)
PO Box 123 Broadway, Ultimo, NSW 2007, Australia
Email: Yan.Li-11@student.uts.edu.au

Jianguo Jack Wang

Faculty of Engineering and Information Technology
University of Technology, Sydney (UTS)
PO Box 123 Broadway, Ultimo, NSW 2007, Australia
Email: Jianguo.Wang@uts.edu.au

Abstract—Zero velocity update (ZUPT) is an effective way for pedestrian navigation in a GPS (Global Positioning System) denied environment. The stance phase in each step provides zero velocity measurement for IMU (Inertial Measurement Unit) drift correction. Most previous research, however, gives navigation solutions only for pedestrian walking but not running. Compared with walking, running has a shorter stance phase with qualified as zero velocity. Therefore a stance phase detector for walking may not be capable for running. This paper presents a novel ZUPT algorithm which can achieve robust pedestrian navigation for walking, stair climbing, and running. Our stance phase detector consists of one footstep detector and two zero velocity detectors (ZVDs). The footstep detector is used to mark each new step, and the first ZVD (ZVD1) can successfully detect zero velocity while walking by setting thresholds on both gyroscope and accelerometer measurements. While ZVD1 is failed for running, the second ZVD (ZVD2) is introduced with a relative larger threshold on gyroscope measurement only. The proposed stance phase detector was tested for walking, running and stair climbing. In all cases, most of the footsteps are detected correctly and our ZUPT algorithm can be successfully implemented. Experimental results show that the navigation accuracy of the proposed algorithm for running cases is comparable to that of walking only cases. Tests on a biped robot are being also conducted to verify the effectiveness of the algorithm.

Keywords- pedestrian navigation; IMU; dead reckoning; ZUPT

I. INTRODUCTION

Seamless navigation in all circumstances, including an environment with degraded GPS signals, is a challenge issue. With the development of robots, their robust tracking and navigation are eagerly demanded. Robots are often deployed in indoor environment where the GPS signal is unreliable. Not dependent on any external information, an IMU can provide continuous navigation information but with accumulated errors, which need to be corrected frequently by other measurements.

Integration of GPS and IMU has got much attention in navigation applications. Developed technologies have made it possible to use GPS in some indoor environments. Godha and Lchappelle proposed a system combined shoe-mounted IMU and GPS to bound drift errors in outdoor scenarios[1]. The system has the ability of using IMU to bridge the navigation

solution indoors and forest environments with severely degraded signal where GPS is unreliable.

There are some non-GPS approaches to track and navigate personal position which normally require external references. Hide and Moore [2] investigated the use of computer vision derived velocity measurements to frequently correct the drift of a low-cost IMU. Hisashi et al. [3] proposed an image sequence matching technique for the recognition of locations and previously visited places. Work is also being done on simultaneous location and mapping (SLAM), which usually uses camera or LIDAR (Light Detection And Ranging) as sensors. However, unlike the inertial sensor, these sensors above are very sensitive to the environment and are unreliable in unfavourable operation conditions.

Many approaches have been developed for pedestrian dead reckoning (PDR) [4]-[18], which does not need additional device except inertial sensors, and can also be applied for pedal robots navigation. The main advantages of inertial sensor-based systems are that they are self-contained, environment-independent and can provide instantaneous position, velocity and attitude measurements. The major challenge for PDR is how to efficiently reduce or bound navigation errors.

There are many different PDR systems using inertial sensors. The simplest one is the pedometer, which counts steps and estimates average length of steps. Cho and Park [4] proposed a pedometer-like approach which uses a two-axis accelerometer and a two-axis magnetometer attached to user's boot. Step length is estimated from accelerometer readings that are passed through a neural network, and a Kalman Filter was used to reduce the effect of magnetic disturbances. While the results in outdoors are reasonable, the results in indoor environment have large errors as the varying magnetic disturbances.

As a special character for pedestrian, there are stance phases during walking, which can be used for PDR drift correction. Therefore, various ZUPT algorithms for PDR navigation have been developed [5-18]. Algorithms for step detection using accelerometers have been presented, which mainly contain three types: peak detection, zero crossing detection and flat zone detection [5]. In [6], a gait state is modelled as a Markov process and gait states are estimated

using the hidden Markov model filter based on force sensors to determine when to apply ZUPT. Similarly, a Markov model is constructed using segmentation of gyroscope outputs in [7]. Slightly different algorithms can be achieved based on both accelerometer and gyroscope outputs. In [8], the zero velocity is determined by comparing z-axis accelerometer and y-axis gyroscope outputs with the threshold value. In [9], the zero velocity is determined based on norms of accelerometer and gyroscope along with variance of accelerometer.

All the above detectors can be generalized as the so-called acceleration moving variance detector, the acceleration magnitude detector, the angular rate energy (ARE) detector which are all generalized likelihood ratio tests. Skog et al. [11] developed a novel stance hypothesis optimal detector; however, it is restricted to 2D cases. Ojeda and Borenstein et al. [12] proposed a shoe-based navigation system consists of a 15-state error model. Their system works well both in 2D and 3D environments. With the ARE detector and related signal processing algorithms, the horizontal relative error was about 0.49% of the total distance travelled, but the vertical error was always more than 1%.

However, all of the algorithms mentioned above fail when operating high-speed movement with the same settings since they are incapable of detecting the stance phase correctly when running. Compared with walking, the duration of stance phase in running is shorter, and the stance phase is less qualifiedly as zero velocity. Barely enlarging the detection threshold will introduce false stance phase detection, which is the last thing wanted in ZUPT.

In this paper, we propose a robust ZUPT algorithm which can correctly detect the stance phase not only while walking, but also running. The novel stance phase detection algorithm includes a footstep detector which indicates every new step, and two zero velocity detectors. The first zero velocity detector (ZVD1) was introduced in our recent research which can correctly detect stance phase while walking and climbing, by setting four conditions on both the accelerometer and gyroscope measurements [21]. The second one (ZVD2) is designed for running based on the motion information of foot dynamics where only gyroscope measurement is used. By strategically combining the three detectors, robust stance phase detection for both walking and running has been achieved. An Extended Kalman Filter (EKF) with 24 error states is then applied for IMU drift correction. Experimental results demonstrate the validity of our robust algorithm. It is better or comparable to some of the highest positioning accuracy figures reported for ZUPT in [12],[13]and [17].

The rest of the paper is organized into five sections. Section II introduces the background of standard strapdown inertial navigation system (INS) mechanism, ZUPT and EKF. Section III details the new stance phase detector which works well for both walking and running. Section IV describes the experiments conducted and their results are analysed and discussed in Section V. The last section is the conclusion and future work.

II. MATHEMATICAL MODELLING

An IMU normally consists of three accelerometers and three gyroscopes in an orthogonal pattern. When it is attached to a moving platform, the standard strapdown INS mechanism is used, as in our system.

A. Strapdown Inertial Navigation Mechanism

Figure 1 shows strapdown INS mechanism. Attitude can be determined by integration of the rotation rate of gyros. After vector transformation, velocity and position can be determined by the integration of acceleration with compensation of gravity and Coriolis force. Details of the INS mechanism are described in [10] and [19].

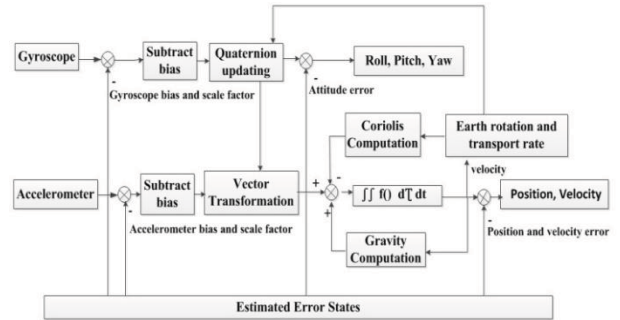


Figure 1. The basic blocks of strapdown INS mechanism

In practice, however, this simple integration will lead to unbounded growth in position errors with time due to the noise associated with the measurement and the non-linearity of the sensors. In order to get high accuracy navigation solution with an IMU, estimated error states with additional measurements and/or constrains are needed in the mechanism to reduce the errors. The technique ZUPT is applied here which utilizes the zero velocity in stance phase as additional measurement to reduce IMU drift.

B. ZUPT

When a person or biped robot walks, its feet alternate between a stance phase and a swing phase. This stance phase appears in each step at zero velocity, thus the velocity of a shoe-mounted IMU can be reset to zero periodically. It is critical to identify the stance phase when the IMU attached to the shoe is stationary and then applies ZUPT to correct the errors with EKF. In each estimation cycle, once zero velocity has been detected, ZUPT delivers new updated error states to the strapdown INS mechanism; otherwise the error states keep unchanged as the ones which are updated in the last stance phase which is usually named as IMU free running. ZUPT can correct velocity directly, and also restrict correlated position and attitude errors and estimating the sensor errors indirectly. Figure 2 shows the main blocks in a typical INS-EKF-ZUPT PDR methodology [9]. It is worth to mention that the miss detection of stance phase will introduce long period of IMU free running which will increase navigation errors, while false detection of stance phase will cause wrongly updated error states which will result in large navigation errors.

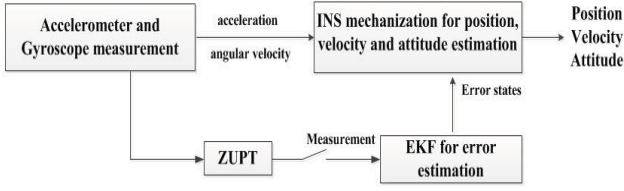


Figure 2. The main blocks in the framework used for pedestrian dead-reckoning

C. Extended Kalman Filter

An exact expression for the system equation of an EKF depends on the states selected and the type of error model used to describe them. The EKF we used includes the following 24 error states [20]:

$$\begin{aligned} \delta x_{Nav} &= [\delta r_N, \delta r_E, \delta r_D, \delta v_N, \delta v_E, \delta v_D, \delta \rho_H, \delta \rho_P, \delta \rho_R]^T \\ \delta x_{INS} &= [\nabla_b, \nabla_f, \varepsilon_b, \varepsilon_f] \\ \delta x_{Grav} &= [\delta g_N, \delta g_E, \delta g_D]^T \end{aligned} \quad (1)$$

Where δx_{Nav} , δx_{INS} and δx_{Grav} are the navigation error vector, the IMU sensor measurement error vector and gravity uncertainty respectively. ∇ is the accelerometer error vector, and ε is the gyro error vector. Subscript b stands for bias and subscript f stands for scale factor.

Psi-angle model is adopted in the system [20]:

$$\begin{aligned} \delta \dot{r} &= -\omega_{en} \times \delta r + \delta v \\ \delta \dot{v} &= -(\omega_{ie} + \omega_{in}) \times \delta v - \delta \rho \times f + \delta g + \nabla \\ \delta \dot{\rho} &= -\omega_{in} \times \delta \rho + \varepsilon \end{aligned} \quad (2)$$

Where, δr , δv and $\delta \rho$ are the position, velocity, and attitude error vectors respectively, δg is the error in the computed gravity vector, f is the specific force vector, ω_{ie} is the earth rotation rate vector, ω_{en} is the transport rate vector and ω_{in} is the angular rate vector from the navigation to the inertial frame.

The dynamic matrix is obtained by a linearization of the equation (2). A detailed expression of the dynamic matrix can be found in [20]. The measurement model is

$$z = H\delta x + n \quad (3)$$

Where $H = [0 \ 1 \ 0 \ 0 \ 0 \ 0 \ 0]$, n is the measurement noise.

Consider the error state, which is the difference between the estimated states computed by the strapdown navigation mechanism and the true state which is zero velocity here.

In this approach, the crucial requirement for achieving a good navigation performance is to get reliable and robust stance phase detection for zero velocity update.

III. STANCE PHASE DETECTION

In order to apply ZUPT, it is critical to identify the stance phase first. Our stance phase detector includes one footstep detector which is used to determine the beginning of the gait cycle and two zero velocity detectors which are used to detect the stance phase for walking and running respectively.

A. Footstep Detector

In pedestrian navigation, it is important to know when the subject takes a step. The step detector can not only mark the beginning of a gait cycle, but also segment the subject's movement into discrete sections. The procedure of segmentation divides a gait cycle into four phases: stance, heel-off, swing, heel strike. The footstep detector mainly detects heel strike after a foot completes swing phase in the air, the foot reaches the highest point and touches down to the ground. Once the heel has hit the ground, the deceleration of the forefoot is very dramatic and characterized by large changes in the acceleration profile. Thus, we simplify the characteristic as that, in heel strike phase, the z-axis acceleration experiences a monotonic decreasing which is unique and obvious to detect so we denote it as a new step.

B. Zero Velocity Detector 1 (ZVD1)

ZVD1 was proposed in our previous study which can effectively detect zero velocity during walking [21]. In the proposed approach, it is not necessary to identify the exact start and end of a stance interval. Rather, as long as one single instance in a stride is detected, it can be used to remove the sensor drift, so the error will not be accumulated. ZVD1 uses both accelerometer and gyro measurements in real-time conditions. The algorithm implemented consists of the following 4 conditions:

- 1) The magnitude of the acceleration a_k , for every sample k:

$$|a_k| = [a_{xk}^2 + a_{yk}^2 + a_{zk}^2]^{0.5} \quad (4)$$

$$C1 = \begin{cases} 1 & th_{a \min} < |a_k| < th_{a \max} \\ 0 & otherwise \end{cases}$$

- 2) The magnitude of the acceleration on z axis $|a_{kz}|$, for every sample k:

$$C2 = \begin{cases} 1 & th_{az \min} < |a_{kz}| < th_{az \max} \\ 0 & otherwise \end{cases} \quad (5)$$

- 3) The magnitude of the gyroscope $|\omega_k|$, for every sample k:

$$|\omega_k| = [\omega_{xk}^2 + \omega_{yk}^2 + \omega_{zk}^2]^{0.5} \quad (6)$$

$$C3 = \begin{cases} 1 & |\omega_k| < th_{\omega \max} \\ 0 & otherwise \end{cases}$$

- 4) The magnitude of the gyroscope on y axis $|\omega_{ky}|$, for every sample k:

$$C4 = \begin{cases} 1 & |\omega_{ky}| < th_{\omega y \max} \\ 0 & otherwise \end{cases} \quad (7)$$

The z axis acceleration and the y axis angular velocity are the most significant indicators of walking event. Since a foot is contacted with ground which indicates a still interval, the acceleration of gravity and the angular rate of foot rotation do not vary over this duration. However, due to unsteady tilt of the shoe surface, the measured ω_y and a_z are not exactly 0 and g respectively, but with large noise. Similarly, although ideally the magnitude of total angular velocity and acceleration on horizontal plane should be zero in a stance phase; but in fact, they will not be zero, but a lower value than a given threshold. The thresholds are based on the average value of the accelerometer and gyro outputs during the initial stationary period of time plus a certain level of fluctuation to ensure its robustness. The initial stationary period is at the beginning of sensor data collection when the IMU is in a stable condition.

These four logical conditions listed as equation (4) to (7) must be satisfied simultaneously to declare a stance phase. Once a zero velocity in one step is detected, velocity is reset to zero; the position, velocity and attitude errors are reset to zero after INS refine the current position, velocity and attitude. The accelerometer and gyro errors and gravity uncertainty are calculated and fed back to the EKF which allows EKF to correct the navigation error afterward.

C. Zero Velocity Detector 2 (ZVD2)

Immediately, it is apparent that the gait cycle of a runner is shorter than that of a walker and that the profile of the gait cycle is significantly different. In the walking gait, the push-off and swing phases are mirrored by the heel strike and stance phases. While one leg is in the push-off phase, the other is in heel strike phase, and while one is in swing phase, the other is in stance phase. This symmetry in the walking gait shows the rhythmical transfer of weight between the two limbs. Conversely, during the running gait this symmetry does not exist. Instead, both legs can be in the swing phase at the same time, and heel strike occurs while the other leg is still in the air [22]

ZVD2 introduced here is specially used to detect zero velocity based on the energy of gyro signals. The zero velocity is determined once “norm (gyro) < E” is satisfied, where E is the threshold of energy ($E_r = 5e-4$ for run, $E_w = 5e-5$ for walk). The process of the stance phase detector is shown in Figure 3.

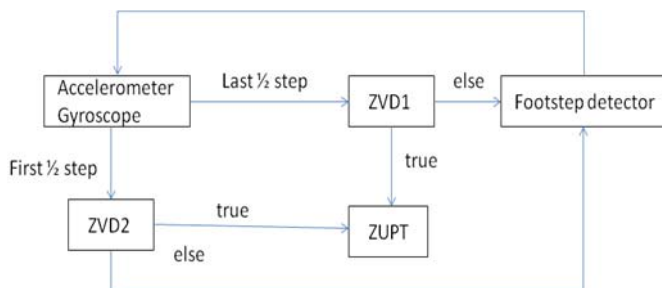


Figure 3. The process of the stance phase detector

Once the footstep detector decides that a new step arrives, in the first half step, we apply both ZVD1 and ZVD2 while the last half step using ZVD1 only. In our case, we do not need to classify the motion is walking or running. Since the threshold for running is larger than that of walking ($E_r > E_w$), in the first half step, as long as the condition for walking is satisfied, we apply E_w afterwards, unless E_w is not satisfied during the whole half step we only apply E_r . For the last half step, ZVD1 is used to prevent some zero-crossings in swing phase mistakenly detected or the case that the foot keeps still for a few seconds. Another swing phase indicator is used to prevent false detection especially when use only measurements of gyroscope.

IV. EXPERIMENTS

A. Hardware Description

We implement the proposed PDR algorithm with a MEMS IMU, Navchip from Intersense Incorporated. Navchip is the smallest IMU in the world and it delivers excellent measurement results. The small size of Navchip makes it easy to attach to a boot and has no effect on walking. Table I lists the specification of Navchip (encapsulated within casing).

TABLE I. SPECIFICATION OF NAVCHIP

Gyroscope Performance		Accelerometer Performance	
Range (deg/sec)	± 480	Range(m/s ²)	± 8
Noise Density (°/s/ $\sqrt{\text{Hz}}$)	0.004	Noise Density (ug/ $\sqrt{\text{Hz}}$)	70
Bias Stability (°/hr, 1 σ)	12	Bias Stability (mg, 1 σ)	0.1

The IMU was mounted on the front surface of a boot. During initial test, we discovered the phenomenon of excessive shock and acceleration measurement overflow. We took countermeasures such as placing shock absorb padding and protective casing. Tests afterwards show reduced shock and improved measurement. Figure 4 shows the accelerometer measurement before (upper figure) and after the shock countermeasure.

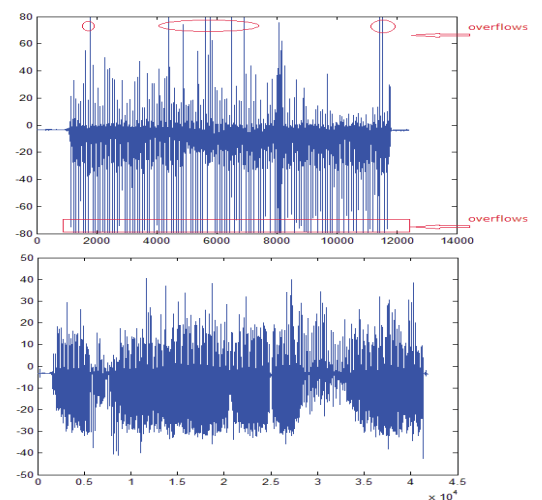


Figure 4. Comparison of acceleration before and after shock reduce

B. Tests

Tests were conducted in three trajectories, as shown in Figure 5, 6 and 7. Each trajectory was tested three times with different human gaits which includes walking, running and walk alternates running. All the trajectories are closed loop, which means the subject stops at the exact same location where he starts. In the figures, the dark dot represents the start point and the blue one is the end point. In addition, in all cases before walking, the subject stands still at the start point for about 4 seconds, which is used in the proposed ZUPT algorithm to measure the IMU attitude in stance phase so as to setting the parameters and initial conditions.

The first two trajectories are conducted on level ground; the last trajectory includes climbing stairs. Trajectory 1 is an “8” shape closed loop that the walking test is conducted for three loops. During our tests, the data will be blocked due to the sensor characteristics when experiencing consecutive overflow, thus our running and walk alternate run tests only follow the trajectory for one and two loops respectively.

Trajectory 2 follows a squared corridor that all the tests are conducted for three loops by another subject. The walking behaviour includes walking, walk alternate run, running and inverse run.

Trajectory 3 extends the 2D environment to 3D which includes climbing stairs. This test combines the three gait behaviours together and during the tests, the subject walks for the first three loops, follows by a three loops’ running, and ends up the tests with randomly walking alternate running for the last three loops.

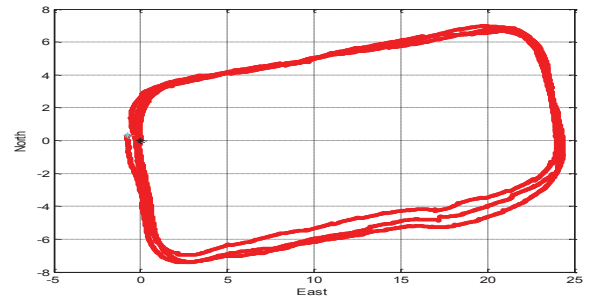


Figure 6. Trajectory 2

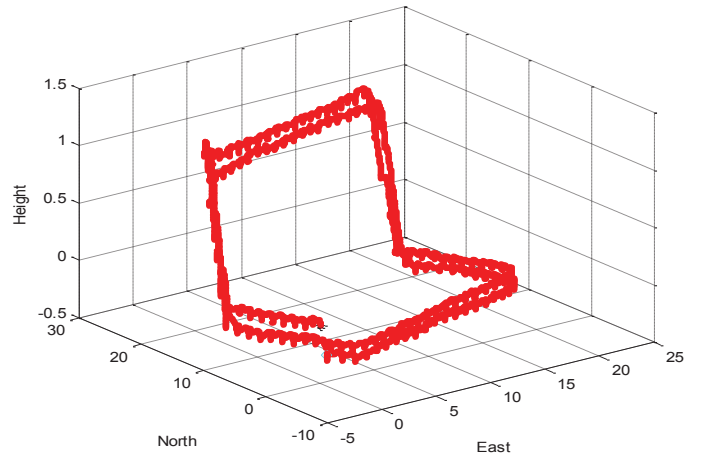


Figure 7. Trajectory 3

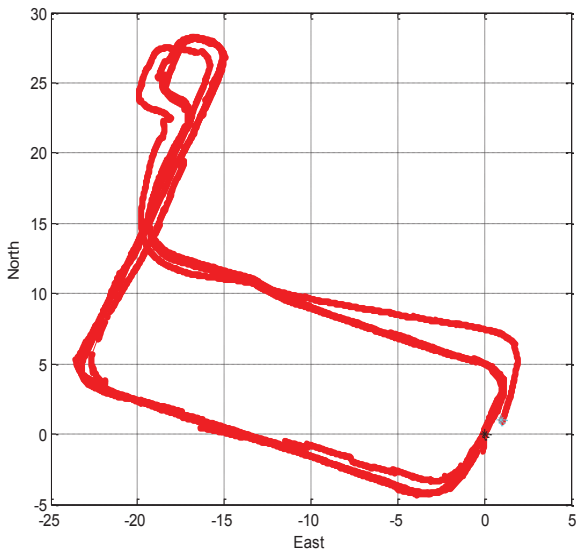


Figure 5. Trajectory 1

V. RESULTS AND DISCUSSION

A. Stance Phase Detection

Figure 8 shows a section of the computed norm of gyro for stance phase detection. The dark dots represent the sample points that are detected to be zero velocity and the diamond indicates a new stride arrives.

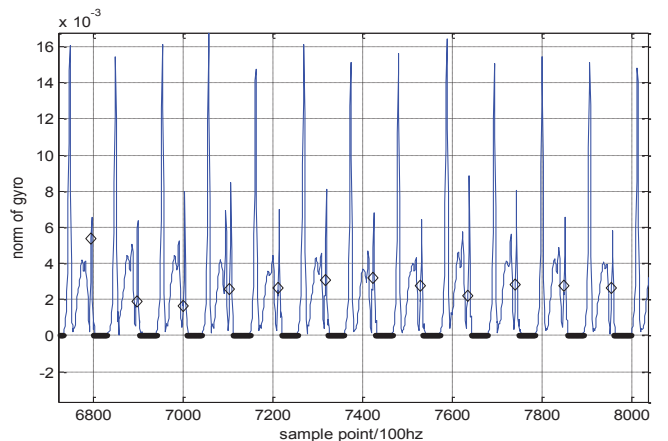


Figure 8. Norm of gyro

B. Navigation Solution

Table II summarises the final return position errors for each trajectory and Table III gives the comparison results of different gait behaviours for same trajectory.

It was expected that the navigation error of running cases should be larger than that of walk alternate running cases since higher dynamics experienced during running shows more variability than in the walking gait, which expressed as fewer ZUPT applies. However, from our results as shown in Table II and Table III, we get different conclusion. The main reason is that when the subject changes his gait randomly, sometimes it's easy to get the footstep detector confused, however, since ZVD1 is applied to prevent false detection in swing phase, we can still get reasonable results.

TABLE II. RETURN POSITION ERRORS

Event		Estimate Distance (m)	Relative error (%)	
			X-Y plane	Z direction
Trajectory1	Walk	288.8	0.49%	8.7e-5%
	Walk & run	171.0	1.22%	0.17%
	Run	89.1	0.87%	0.0015%
Trajectory2	Walk	192.2	0.28%	1.9e-5%
	Walk & run	192.8	0.86%	0.037%
	Run	192.2	0.29%	5.5e-4%
	Inverse run	187.4	1.22%	0.001%
Trajectory3	Walk & run	525.6	0.50%	0.38%
Average		229.9	0.72%	0.074%

TABLE III. ERRORS OF GAIT BEHAVIOUR

	Relative error (%)	
	X-Y plane	Z direction
Walk	0.39%	5.3e-5%
Walk & run	1.04%	0.21%
Run	0.79%	0.001%

Here we segment the last test into three segments since each gait maintains for three loops and always back to the start point after each loop. In the X-Y plane, the red line draws the first three walking loops; the green line represents the running loops while the blue one is the trajectory conducted by walking alternate running. The figures also demonstrate the same results as table III that the running performance is better than that of walk alternate running.

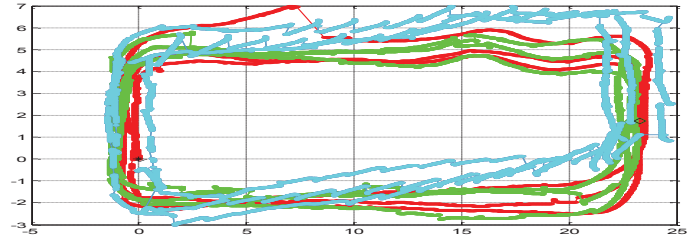


Figure 9. Trajectory3 including all gaits

In addition, out of the excessive shock, the bi-directional overflow will affect the accuracy in a large extent, although we have already taken measures to reduce the impact, it is still inevitable that the overflow would affect INS mechanism computing vertical velocity and position. Figure 4 shows the effectiveness of shock reduction for walking behaviour, the figure below indicates that our current protective measure is not enough capable of running. In figure 10, the z-axis acceleration is severely overflowed that we are considering using other large range sensors to do the tests. X-axis represents the sample times. The diamond here is the detection of new step by footstep detector, while the black dots are the sample points that have been detected to be zero velocity.

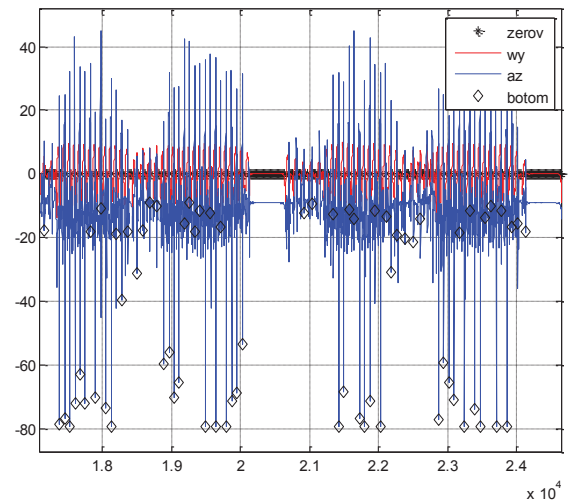


Figure 10. Raw accelerometer data

VI. CONCLUSION AND FUTURE WORK

This paper presented a robust algorithm for self-contained PDR system which can handle running cases. From the test results, we can draw a conclusion that the algorithm is efficient to limit the growth of IMU error. Our robust stance phase detection shows satisfactory performance. This real-time algorithm could give accurate navigation solution simultaneously as a pedal robots or pedestrian is walking or running.

The proposed algorithm performs well in both walking or running conditions, however, due to the excessive shock and sensor measurement overflow, there still exist many problems and has room to improve. We are still working on that. In the

future, we will develop methods that can handle the overflow and a more efficient robust running algorithm. Currently tests on a biped robot are also being conducted to verify the effectiveness of the algorithm.

ACKNOWLEDGMENT

The authors sincerely appreciate Professor Guang Hong for providing the sensor as well as the UTS workshop personals for manufacturing the protective casing of the IMU sensor.

REFERENCES

- [1] S. Godha and G. Lachapelle, "Foot mounted inertial system for pedestrian navigation," *Meas. Sci. Technol.*, vol. 19 2008.
- [2] C. Hide, et al., "Low Cost Vision-Aided IMU for Pedestrian Navigation," *Global Positioning Systems*, vol. 10, pp. 3-10, 2011.
- [3] B. Schiele, et al., "Realtime Personal Positioning System for Wearable Computer," presented at the 3rd IEEE International Symposium on Wearable Computers (ISWC 1999), Washington, DC, USA 1999.
- [4] S. Y. Cho and C. G. Park, "MEMS Based Pedestrian Navigation System", *Journal of Navigation*, vol. 59, pp. 135-153, 2006.
- [5] S. Y. Cho, et al., "A Personal Navigation System Using Low-Cost MEMS/GPS/Fluxgate", presented at the Proceedings of the 59th Annual Meeting of The Institute of Navigation and CIGTF 22nd Guidance Test Symposium, Albuquerque, NM, 2003.
- [6] Y. S. Suh and S. Park, "Pedestrian inertial navigation with gait phase detection assisted zero velocity updating", presented at the Autonomous Robots and Agents, 2009. ICARA 2009. 4th International Conference on Autonomous Robots and Agents, Wellington, New Zealand, 2009.
- [7] S. K. Park and Y. S. Suh, "A Zero Velocity Detection Algorithm Using Inertial Sensors for Pedestrian Navigation Systems", *Sensors* vol. 10, pp. 9163-9178, 2010.
- [8] X. Yun, et al., "Self-contained Position Tracking of Human Movement Using Small Inertial/Magnetic Sensor Modules", presented at the 2007 IEEE International Conference on Robotics and Automation, Roma, Italy, 2007.
- [9] A. R. Jiménez, et al., "Indoor pedestrian navigation using an INS/EKF framework for yaw drift reduction and a foot-mounted IMU", presented at the 7th Workshop on Positioning Navigation and Communication (WPNC), Dresden 2010.
- [10] E. Foxlin, "Pedestrian Tracking with Shoe-Mounted Inertial Sensors", *IEEE Computer Graphics and Applications In Computer Graphics and Applications*, vol. 25, pp. 38-46, November 2005.
- [11] I. Skog, et al., "Evaluation of zero-velocity detectors for foot-mounted inertial navigation systems", presented at the 2010 International Conference on Indoor Positioning and Indoor Navigation (IPIN), Zurich 2010.
- [12] L. Ojeda and J. Borenstein, "Non-GPS Navigation for Security Personnel and First Responders", *Journal of Navigation*, vol. 60, pp. 391-407, 09 August 2007.
- [13] N. Castañeda and S. Lamy-Perbal, "An improved shoe-mounted inertial navigation system", in 2010 International Conference on Indoor Positioning and Indoor Navigation (IPIN), Campus Science City, ETH Zurich, 2010.
- [14] C. Huang, et al., "Synergism of INS and PDR in Self-Contained Pedestrian Tracking With a Miniature Sensor Module", *Sensors Journal*, IEEE vol. 10, pp. 1349-1359, Aug. 2010.
- [15] R. Feliz, et al., "Pedestrian Tracking Using Inertial Sensors", *Journal of Physical Agents*, vol. 3, pp. 35-43, Jan-2009.
- [16] S. Rajagopal, "Personal dead reckoning system with shoe mounted inertial sensors", Master of Science, Electrical and Electronic Engineering KTH, Stockholm, Sweden, 2008.
- [17] O. Bebek, et al., "Personal Navigation via High-Resolution Gait-Corrected Inertial Measurement Units", presented at the IEEE Transactions on Instrumentation and Measurement, 2010.
- [18] A. R. Jimenez, et al., "A Comparison of Pedestrian Dead-Reckoning Algorithms Using a Low-Cost MEMS IMU", *IEEE International Symposium on Intelligent Signal Processing*, 2009 pp. 37 - 42 26-28, Aug 2009.
- [19] H. K. Lee, "Integration of GPS/Pseudolite/INS for High Precision Kinematic Positioning and Navigation", Doctor of Philosophy, School of Surveying and Spatial Information Systems, The University of New South Wales, Sydney NSW 2052, Australia, 2004.
- [20] Dorota. A, et al., "Bridging GPS Gaps in Urban Canyons: Can ZUPT Really Help?," *Proceedings of the 58th Annual Meeting of The Institute of Navigation and CIGTF 21st Guidance Test Symposium*, pp. 231-240, June 24 - 26 2002.
- [21] Yan. Li, et al., "A Robust Humanoid Robot Navigation Algorithm with ZUPT", presented at the IEEE International Conference on Mechatronics and Automation, 2012.
- [22] Sidney. Kwakkel, "Human Lower Limb Kinematics Using GPS/INS", Master of Philosophy, Department of Geomatics Engineering, The University of Calgary, December, 2008.